Isolation of a perfectly linear uranium(II) metallocene

Fu-Sheng Guo,[a] Nikolaos Tsoureas,[a] Guo-Zhang Huang,[b] Ming-Liang Tong,*[b] Akseli Mansikkamäki,*[c] and Richard A. Layfield*[a]

In memory of Professor Richard A. Andersen

Abstract: Reduction of the uranium(III) metallocene [(η^5-C$_5$^{i}Pr$_5$)$_2$UI] (**1**) with potassium graphite produces the 'second-generation' uranocene [(η^5-C$_5$^{i}Pr$_5$)$_2$U] (**2**), which contains uranium in the formal divalent oxidation state. The geometry of **2** is that of a perfectly linear bis(cyclopentadienyl) sandwich complex, with the ground-state valence electron configuration of uranium(II) revealed by electronic spectroscopy and density functional theory to be 5f^3 6d^1. Appreciable covalent contributions to the metal-ligand bonds were determined from a computational study of **2**, including participation from the uranium 5f and 6d orbitals. Whereas three unpaired electrons in **2** occupy orbitals with essentially pure 5f character, the fourth electron resides in an orbital defined by strong 7s-6d$_{z2}$ mixing.

Metallocenes play a pivotal role in the development of organometallic chemistry. The most studied members of the family are metallocenes of the transition metals, the reactivity and properties of which are remarkably diverse, leading to widespread applications in established areas such as olefin polymerization catalysis[1] and polymer chemistry,[2,3] whilst also accounting for new developments in small-molecule activation[4,5] and redox-active materials.[6,7] Metallocenes are also prominent in f-element chemistry owing to their distinct catalytic and stoichiometric reactivity,[8,9] and for their ability to provide platforms for the study of fundamental aspects of chemical bonding in lanthanide and actinide compounds.[10] Recently, metallocenes of certain anisotropic lanthanides have risen to prominence as high-performance single-molecule magnets.[11–13]

The most iconic form of a metallocene, *i.e.* the *bis*(cyclopentadienyl) sandwich [(η^5-Cp^R)$_2$M] (R denotes various organic substituents), is known for many metals in the s-, p- and d-blocks of the periodic table,[14] as it is for some lanthanides.[15–17] For the actinide series, the same sandwich structural motif is unknown, which is presumably due to the instability of the divalent form of these elements with respect to oxidation. If such actinide metallocenes could be synthesized, not only would they incorporate the 5f elements into the wider metallocene family, they would also furnish new insight into the bonding in actinide compounds and for developing new reactivity based on highly reducing divalent actinides. Recently, it has been shown that stable, molecular compounds of divalent actinides, particularly uranium, can be synthesized by reduction of trivalent precursors.[18–23] Therefore, it occurred to us that a uranocene of the type [(η^5-Cp^R)$_2$U] should be accessible by the action of a strong reducing agent on an appropriate uranium(III) metallocene precursor. To that end, a reductive salt-metathesis reaction of the previously reported uranium(III) compound [(η^5-C$_5$^{i}Pr$_5$)$_2$UI] (**1**)[24] with a slight excess of potassium graphite was undertaken, which yielded the desired divalent uranocene [(η^5-C$_5$^{i}Pr$_5$)$_2$U] (**2**) according to Scheme 1.

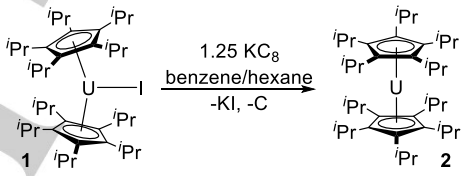

Scheme 1. Synthesis of the divalent uranocene [(η^5-C$_5$^{i}Pr$_5$)$_2$U] (**2**).

Following work-up, compound **2** was crystallized as a benzene solvate (**2**·2C$_6$H$_6$) and isolated as very dark green crystals (appearing black to the eye) in reproducible yields of ~30%. The molecular structure of **2** was revealed by X-ray crystallography to contain *bis*(cyclopentadienyl)uranium units with the uranium atom occupying a crystallographic inversion centre (Figure 1, Table S1). Hence, the two ligands in **2** adopt a staggered conformation reminiscent of the D_{5d} polymorph of ferrocene,[25] with the isopropyl groups resulting in molecular C_s symmetry.

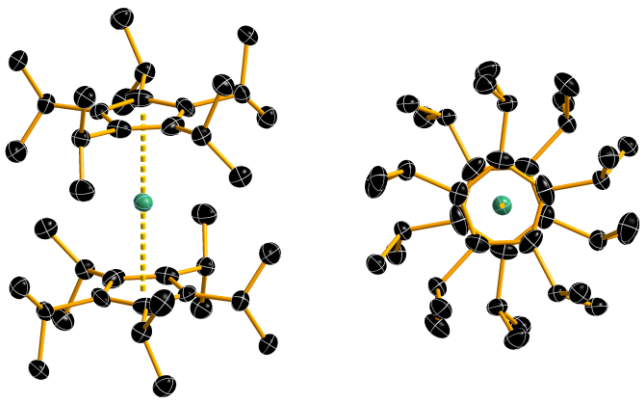

Figure 1. Thermal ellipsoid representations (50% probability) of the molecular structure of **2**. For clarity, the hydrogen atoms are omitted.

[a] Dr F.-S. Guo, Dr N. Tsoureas, Prof. Dr R. A. Layfield
Department of Chemistry
University of Sussex
Falmer, Brighton, BN1 9QR (U.K.)
E-mail: R.Layfield@sussex.ac.uk
[b] G.-Z. Huang, Prof. Dr M.-L. Tong
Key Laboratory of Bioinorganic and Synthetic Chemistry of the Ministry of Education, School of Chemistry
Sun Yat-Sen University
E-mail: tongml@mail.sysu.edu.cn
Guangzhou 510275 (P.R. China)
[c] Dr A. Mansikkamäki
Department of Chemistry, Nanoscience Center
University of Jyväskylä
P.O. Box 35, Jyväskylä, FI-40014 (Finland)
E-mail: Akseli.Mansikkamaki@jyu.fi

Supporting information for this article is given via a link at the end of the document.

The range of U–C distances in **2** is 2.756(4)-2.804(4) Å with a U–Cp_{cent} distance of 2.504(1) Å, the latter being slightly longer than the analogous distance of 2.472(3) Å in the previously reported uranium(III) metallocene cation $[(\eta^5\text{-}C_5{}^i\text{Pr}_5)_2\text{U}]^+$ (**3**). Since the uranium atom in **2** occupies a crystallographic inversion centre the Cp-U-Cp angle is 180.0°, which is markedly wider than the angle of 167.82(8)° in **3**.

To gain insight into the valence electron configuration of **2**, the UV/vis/NIR spectra were recorded at two concentrations. The spectra (Figures 2, S5, S6) feature a shoulder at 320 nm and broad absorptions in the region λ = 550-750 nm with local maxima at 572 and 642 nm (Figure 2), which is significant because the analogous spectra for **1** and **3** do not feature any significant absorptions at wavelengths longer than 500 nm.

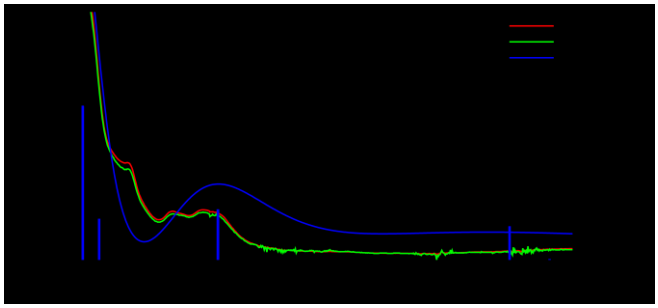

Figure 2. The measured UV/vis/NIR spectra of compound **2** in hexane along with the spectrum simulated based on TDDFT results. The vertical bars show TDDFT oscillator strengths of the individual transitions.

The spectrum was interpreted with the aid of time-dependent DFT (TDDFT) calculations as performed on an optimized geometry of **2**. The simulated spectrum is show in Figure 2 and details of the excitations are given in Table S2. The shape of the measured UV/vis/NIR spectrum is reasonably well reproduced considering the usual errors margins in TDDFT calculations. The spectrum shows very few features, which is most likely a result of the molecular inversion symmetry and the near-perfect S_{10} symmetry in solution, which greatly reduces the number of allowed transitions. The two main features of the calculated spectrum are a shoulder at 363 nm and a band at 676 nm. The shoulder is much clearer in the measured spectrum than in the simulated one. Both features arise from two almost perfectly degenerate transitions. The 363 nm transition consists of the transfer of an electron from the near-degenerate ligand HOMOs to the δ-symmetric $6d_{x^2-y^2}$ and $6d_{xy}$ orbitals. The calculated band at 676 nm corresponding to the experimental λ_{max} at 642 nm, arises from excitations from the HOMO to vacant 5f orbitals. This latter transition is significant as it supports the existence of the $5d^3\ 6d^1$ configuration and thus the formal divalent oxidation state of uranium. The electron configuration of **2** is therefore similar to that of the previously reported uranium(II) complex $[U(\eta^5\text{-}C_5H_4SiMe_3)_3]^-$,[21] as opposed to the $5f^4$ configuration observed in two other examples.[18,19]

To gain further insight into the electronic structure and bonding in **2**, a density functional theory (DFT) calculation was performed on the geometry of the molecule in the experimentally determined C_s symmetry. The results show that the ground-state configuration is indeed $5f^3\ 6d^1$, which has A_g symmetry. The $5f^4$ configuration corresponds to the lowest state in the A_u symmetry and lies 8908 cm^{-1} above the ground configuration. The presence of a crystallographic inversion centre in **2** means that any mixing of states arising from the two different configurations is strictly forbidden.

The orbital interactions in **2** are schematically represented in Figure 3. The main covalent contribution arises from dative electron donation from the HOMOs of the cyclopentadienyl ligands to the vacant uranium 6d orbitals, with the resulting bonding orbitals showing 13-17% 6d character. A small but non-negligible amount of covalency also arises from mixing of the ligand HOMOs and the uranium 5f orbitals, which is weak and the resulting orbitals have only 4-6% 5f character. The three singly occupied orbitals housing the unpaired 5f electrons have more than 96% 5f character each. The 6d orbital with one unpaired electron has 54% 7s character but only 40% 6d character. The strong mixing of the $6d_{z^2}$ and 7s orbitals in **2** leads to an orbital with large spatial extent in the empty equatorial region between the Cp ligands. The presence of this non-bonding 6d/7s orbital is most likely the reason why the Cp-U-Cp angle in **2** is perfectly linear. The lowest unoccupied orbitals are the δ-symmetric $6d_{xy}$ and $6d_{x^2-y^2}$ orbitals. Our results on **2** are consistent with a recently reported theoretical study on the same compound but considered in the closely related S_{10}-symmetric form.[26]

The bent metallocene structural motif is well known in early actinide chemistry, particularly for uranium(IV) and uranium(III) in compounds with the general formula $[Cp_2UX_2]$ and $[Cp_2UX(L)_n]$ (X = anionic ligand, L = neutral Lewis base).[27] The ubiquitous nature of actinide metallocenes with non-parallel cyclopentadienyl ligands therefore means that Berthet's uranium(IV) complex cation $[(Cp^*)_2U(NCMe)_5]^{2+}$ is a remarkably rare species in which the Cp* ligands are co-parallel, with the acetonitrile ligands adopting a pentagonal arrangement in the equatorial plane.[28] The geometry of this axially symmetric uranium(IV) metallocene is thought to be enforced by steric interactions between the various ligand substituents, which contrasts to the explanation for the linear geometry of **2**, where an unusual mixing of the uranium 7s and 6d orbitals plays the dominant structure-directing role. As such, **2** occupies a unique position amongst the large family of actinide metallocenes in being structurally more reminiscent of a d-block metallocene.[29] The role of orbital effects in determining the geometry of linear uranium sandwich complexes with parallel, η-bonded ligands has been studied in detail for the famous 'first-generation' uranocene $[U(\eta^8\text{-}C_8H_8)_2]$[30,31] and has also been observed in the cycloheptatrienyl analogue $[U(\eta^7\text{-}C_7H_7)_2]^-$.[32] The structure of **2** is evocative of its more established cousins, however the mixed $5d^3\ 6d^1$ configuration is a distinctive feature of this 'second-generation' uranocene.

The molar magnetic susceptibility (χ_M) as a function of temperature was determined on a polycrystalline sample of **2** in the temperature range 2-300 K using applied fields of 1 kOe and 5 kOe (Figures S7-S9). At 5 kOe, the value of $\chi_M T$ at 290 K was determined to be 0.96 $cm^3\ K\ mol^{-1}$, which corresponds to μ_{eff} = 2.78 μ_B. On lowering the temperature, $\chi_M T$ gradually decreases down to 25 K before undergoing a precipitous drop and reaching 0.47 $cm^3\ K\ mol^{-1}$ at 2 K (μ_{eff} = 1.95 μ_B). The overall

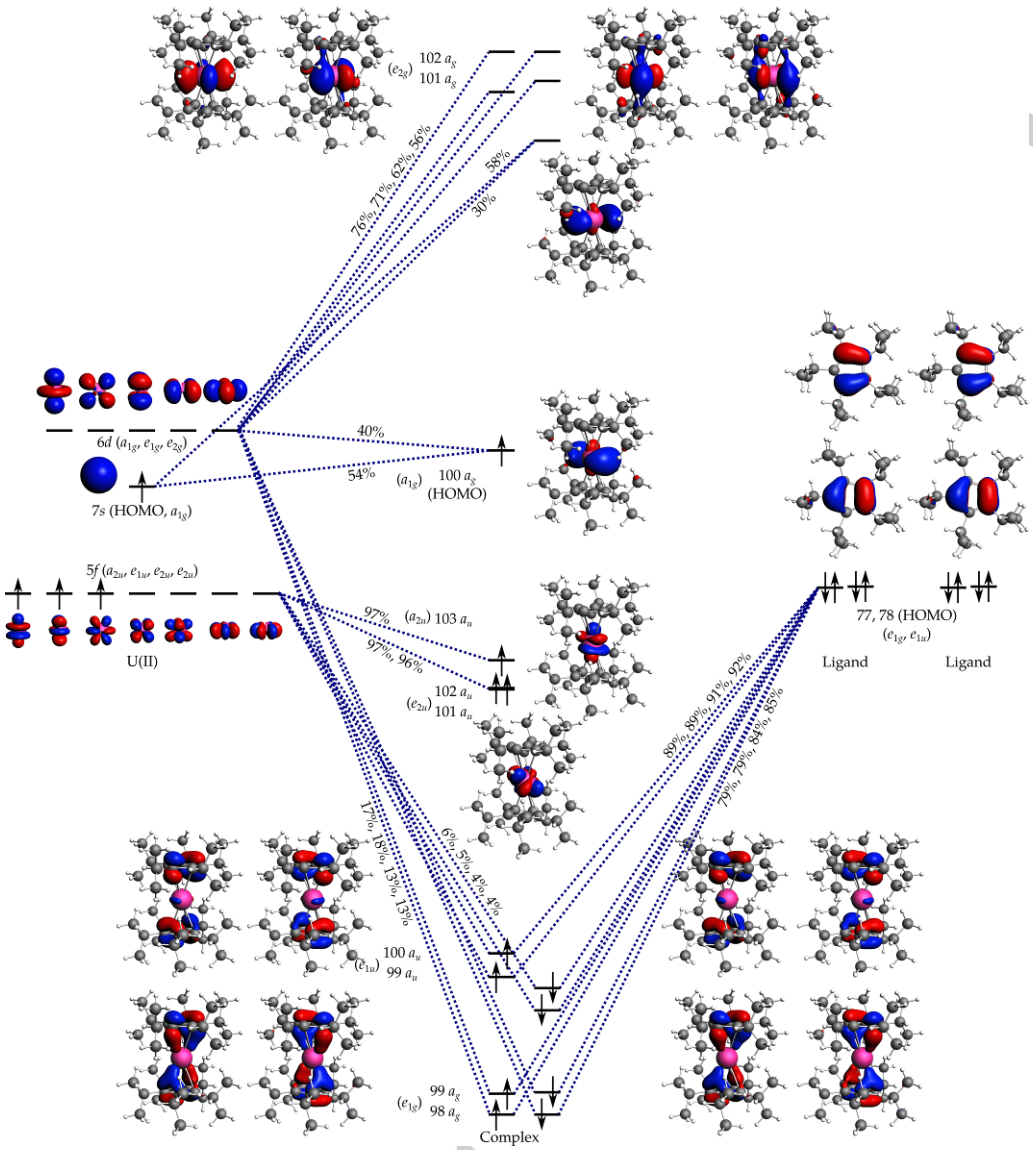

Figure 3. MO diagram for **2**. The symmetry species of the orbitals are given both in the actual C_s symmetry and in the approximate S_{10} symmetry in parenthesis. The percentage numbers give the contributions from the various fragment orbitals to the MOs.

temperature dependence of $\chi_M T$ for **2** contrasts somewhat with those observed for other divalent uranium compounds, in which the susceptibility decreases more rapidly at higher temperatures and experiences only a slight drop at lower temperatures.[18–21] This difference may be explained by the high symmetry of the uranium geometry in **2**, which is clearly very different to the low symmetry of the other divalent uranium compounds.

AC magnetic susceptibility measurements were also performed on **2** in order to search for slow relaxation properties. No maxima were observed in the temperature-dependence of the out-of-phase susceptibility in zero applied DC field nor in applied fields of 1 kOe and 3 kOe when using various frequencies up to 1488 Hz (Figures S10-S12). Thus, like its trivalent analogues **1** and **3**, compound **2** does not show single-molecule magnet behaviour. In the case of **1** and **3**, this is a consequence of covalency effects arising from interactions of the uranium 5f orbitals with the ligands, which partially quenches the orbital contribution to the magnetic moment, leading to strong mixing of various M_J states belonging to low-lying multiplets.[24,33] The same arguments also hold for **2**, but here the situation is more complicated. In addition to the crystal-field splitting of the states arising from the 5f configuration, **2** also has additional interactions arising from the Coulomb and exchange interaction between the 5f and 6d/7s electrons, which leads to additional splitting and mixing within the low-lying multiplets.

Stable, molecular lanthanide and actinide compounds in which the metal occupies an unusual oxidation state have provided valuable insight into the chemistry of this fascinating

family of elements.[34–36] The relative ease with which the divalent uranocene **2** can be synthesized from **1** using a standard reducing agent raises the question 'can compound **2** itself be reduced to give a monovalent, uranium(I) compound?'. To explore this question, cyclic voltammetry (CV) was performed on **1** in THF using $[N^nBu_4][BPh_4]$ as the electrolyte and decamethylferrocene (Fc*) as the internal reference.[37] The measurement showed three independent processes that are stable over at least six cycles, with two irreversible processes at $E_{1/2}$ = –0.608 V and –1.900 V versus $[Fc^*]/[Fc^*]^+$ and a quasi-reversible process at approximately –2.85 V (see SI full details, Figures S13-S15 and Tables S3-S5). The first irreversible process at –0.608 V can attributed to the U(IV)/U(III) redox couple and the second process to the U(III)/U(II) couple. The third process at –2.85 V can be tentatively assigned to a U(II)/U(I) redox couple. A cathodic current response was also observed at –3.08 V (close to the solvent breakdown window), which could indicate a highly reactive U(I) species undergoing decomposition on the electrochemical timescale (Figure S15). These studies suggest that a monovalent uranium(I) metallocene may not evade capture under chemical reduction conditions for too long.

In summary, the second-generation uranocene $[(\eta^5\text{-}C_5{}^iPr_5)_2U]$ (**2**) was synthesized and found to possess a perfectly linear geometry with parallel cyclopentadienyl ligands. Electronic spectroscopy and DFT calculations revealed the ground-state valence electron configuration of the divalent uranium centre in **2** to be $5f^3\ 6d^1$. The chemical bonding in **2** features an appreciable degree of covalency and includes contributions from the uranium 5f and 6d orbitals, with a singly-occupied, non-bonding $6d_{z^2}$-7s hybrid orbital being responsible for the observed geometry of the complex. The appreciable radial extension of this hybrid orbital implies that **2** should have interesting chemistry as a reducing agent, which our future efforts will focus on.

Acknowledgements

We thank the ERC (CoG 646740), the EPSRC (EP/M022064/1), the NSF China (projects 21620102002, 91422302), the National Key Research and Development Program of China (2018YFA0306001), the Magnus Ehrnrooth Foundation, the CSC-IT Center for Science in Finland, the Finnish Grid and Cloud Infrastructure (urn:nbn:fi:research-infras-2016072533), and Prof. H. M. Tuononen (University of Jyväskylä) for computational resources.

Keywords: uranium • metallocenes • chemical bonding • electronic structure • magnetic properties

[1] M. Stürzel, S. Mihan, R. Mülhaupt, *Chem. Rev.* **2016**, *116*, 1398.
[2] R. A. Musgrave, A. D. Russell, D. W. Hayward, G. R. Whittell, P. G. Lawrence, P. J. Gates, J. C. Green, I. Manners, *Nat. Chem.* **2017**, *9*, 743.
[3] Y. Sha, Y. Zhang, E. Xu, C. W. McAlister, T. Zhu, S. L. Craig, C. Tang, *Chem. Sci.* **2019**, *10*, 4959.
[4] M. J. Chalkley, T. J. Del Castillo, B. D. Matson, J. C. Peters, *J. Am. Chem. Soc.* **2018**, *140*, 6122.
[5] M. J. Chalkley, P. H. Oyala, J. C. Peters, *J. Am. Chem. Soc.* **2019**, *141*, 4721.
[6] Y. Ding, Y. Zhao, Y. Li, J. B. Goodenough, G. Yu, *Energy Environ. Sci.* **2017**, *10*, 491.
[7] P. J. Celis-Salazar, M. Cai, C. A. Cucinell, S. R. Ahrenholtz, C. C. Epley, P. M. Usov, A. J. Morris, *J. Am. Chem. Soc.* **2019**, *141*, 11947.
[8] F. Allouche, K. W. Chan, A. Fedorov, R. A. Andersen, C. Copéret, *Angew. Chemie* **2018**, *130*, 3489.
[9] D. B. Culver, W. Huynh, H. Tafazolian, T.-C. Ong, M. P. Conley, *Angew. Chemie Int. Ed.* **2018**, *57*, 9520.
[10] C. Zhang, G. Hou, G. Zi, W. Ding, M. D. Walter, *J. Am. Chem. Soc.* **2018**, *140*, 14511.
[11] C. A. Gould, K. R. McClain, J. M. Yu, T. J. Groshens, F. Furche, B. G. Harvey, J. R. Long, *J. Am. Chem. Soc.* **2019**, *141*, 12967.
[12] F.-S. Guo, B. M. Day, Y.-C. Chen, M.-L. Tong, A. Mansikkamäki, R. A. Layfield, *Science.* **2018**, *362*, 1400.
[13] B. M. Day, F.-S. Guo, R. A. Layfield, *Acc. Chem. Res.* **2018**, *51*, 1880.
[14] P. Jutzi, N. Burford, *Chem. Rev.* **1999**, *99*, 969–990.
[15] M. Schultz, C. J. Burns, D. J. Schwartz, R. A. Andersen, *Organometallics* **2000**, *19*, 781.
[16] P. B. Hitchcock, J. A. K. Howard, M. F. Lappert, S. Prashar, *J. Organomet. Chem.* **1992**, *437*, 177.
[17] W. J. Evans, L. A. Hughes, T. P. Hanusa, *Organometallics* **1986**, *5*, 1285.
[18] B. S. Billow, B. N. Livesay, C. C. Mokhtarzadeh, J. McCracken, M. P. Shores, J. M. Boncella, A. L. Odom, *J. Am. Chem. Soc.* **2018**, *140*, 17369.
[19] H. S. Lapierre, A. Scheurer, F. W. Heinemann, W. Hieringer, K. Meyer, *Angew. Chemie - Int. Ed.* **2014**, *53*, 7158.
[20] C. J. Windorff, M. R. MacDonald, K. R. Meihaus, J. W. Ziller, J. R. Long, W. J. Evans, *Chem. Eur. J.* **2016**, *22*, 772.
[21] M. R. MacDonald, M. E. Fieser, J. E. Bates, J. W. Ziller, F. Furche, W. J. Evans, *J. Am. Chem. Soc.* **2013**, *135*, 13310.
[22] J. Su, C. J. Windorff, E. R. Batista, W. J. Evans, A. J. Gaunt, M. T. Janicke, S. A. Kozimor, B. L. Scott, D. H. Woen, P. Yang, *J. Am. Chem. Soc.* **2018**, *140*, 7425.
[23] C. J. Windorff, G. P. Chen, J. N. Cross, W. J. Evans, F. Furche, A. J. Gaunt, M. T. Janicke, S. A. Kozimor, B. L. Scott, *J. Am. Chem. Soc.* **2017**, *139*, 3970.
[24] F.-S. Guo, Y.-C. Chen, M.-L. Tong, A. Mansikkamäki, R. A. Layfield, *Angew. Chemie Int. Ed.* **2019**, *58*, 10163.
[25] J. D. Dunitz, L. E. Orgel, A. Rich, *Acta Crystallogr.* **1956**, *9*, 373.
[26] J. Yu, F. Furche, **2019**, DOI 10.26434/chemrxiv.9640931.v1.
[27] R. R. Langeslay, C. J. Windorff, M. T. Dumas, J. W. Ziller, W. J. Evans, *Organometallics* **2018**, *37*, 454.
[28] J. Maynadié , J.-C. Berthet, P. Thuéry, M. Ephritikhine, *J. Am. Chem. Soc.* **2006**, *128*, 1082.
[29] C. Elschenbroich, *Organometallics. 3rd Ed.*, Wiley-VCH, Weinheim, Germany, **2006**.
[30] A. Streitwieser, U. Mueller-Westerhoff, *J. Am. Chem. Soc.* **1968**, *90*, 7364.
[31] D. Seyferth, *Organometallics* **2004**, *23*, 3562.
[32] T. Arliguie, M. Lance, M. Nierlich, J. Vigner, M. Ephritikhine, *J. Chem. Soc., Chem. Commun.* **1995**, 183.
[33] L. Escalera-Moreno, J. J. Baldoví, A. Gaita-Ariño, E. Coronado, *Inorg. Chem.* **2019**, *58*, 11883.
[34] P. B. Hitchcock, M. F. Lappert, L. Maron, A. V. Protchenko, *Angew. Chem. Int. Ed.* **2008**, *47*, 1488.
[35] C. T. Palumbo, I. Zivkovic, R. Scopelliti, M. Mazzanti, *J. Am. Chem. Soc.* **2019**, *141*, 9827.
[36] N. T. Rice, I. A. Popov, D. R. Russo, J. Bacsa, E. R. Batista, P. Yang, J. Telser, H. S. La Pierre, *J. Am. Chem. Soc.* **2019**, *141*, 13222.
[37] C. J. Inman, F. G. N. Cloke, *Dalton Trans.* **2019**, *48*, 10782.

Entry for the Table of Contents

COMMUNICATION

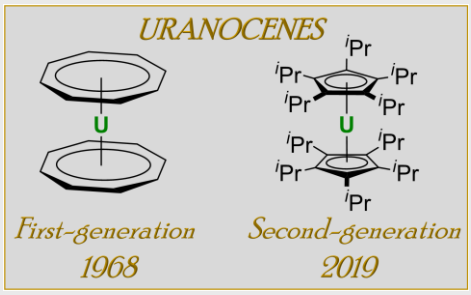

Fu-Sheng Guo, Nikolaos Tsoureas, Guo-Zhang Huang, Ming-Liang Tong, Akseli Mansikkamäki,* Richard A. Layfield*[a]*

Page No. – Page No.

Isolation of a perfectly linear uranium(II) metallocene